Materials Science and Engineering A 506 (2009) 187–190

Contents lists available at ScienceDirect

Materials Science and Engineering A

journal homepage: www.elsevier.com/locate/msea

Short communication

In situ neutron-diffraction study of tensile deformation of a bulk nanocrystalline alloy

G.J. Fan[a,*], L. Li[a], Bin Yang[b], H. Choo[a], P.K. Liaw[a], T.A. Saleh[c], B. Clausen[c], D.W. Brown[c]

[a] Department of Materials Science and Engineering, The University of Tennessee, Knoxville, TN 37996, USA
[b] State Key Laboratory for Advanced Metals and Materials, University of Science and Technology Beijing, Beijing 100083, China
[c] Los Alamos Neutron Science Center, Los Alamos National Laboratory, Los Alamos, NM 87545, USA

ARTICLE INFO

Article history:
Received 4 May 2008
Received in revised form 8 November 2008
Accepted 21 November 2008

Keywords:
Plastic deformation
Nanocrystalline materials
Neutron-diffraction

ABSTRACT

In situ neutron-diffraction technique has been employed to study the uniaxial tensile deformation of a bulk nanocrystalline Ni–Fe alloy. In contrast to an increase in the full-width half-maximum (FWHM) of the neutron-diffraction patterns for the coarse-grained Ni, the FWHM for the nanocrystalline Ni–Fe alloy decreases with increasing the plastic strain, ε_P. The deformation with $\varepsilon_P < 1.5\%$ did not introduce a residual lattice strain and a texture in the nanocrystalline Ni–Fe alloy, which were otherwise developed in the coarse-grained Ni.

Extensive efforts have been made to explore the deformation mechanisms of nanocrystalline (nc) metals and alloys with grain sizes less than 100 nm [1–11]. Previous studies, primarily based on the molecular dynamics (MD) simulations and transmission electron microscopy (TEM) observations [5–16], have suggested that various competing deformation mechanisms, i.e., grain-boundary (GB) sliding, dislocation motion, mechanical twinning, may be responsible for the observed plasticity in nc metals and alloys, in contrast to the dislocation pile-ups at the grain boundaries for their coarse-grained (cg) counterparts. Recently, both in situ and ex situ X-ray diffraction techniques were employed to monitor the structural evolutions in nc metals and alloys during the plastic deformation [17–21]. The results indicate that dislocation motions play a role during the plastic deformation of nc metals and alloys, which is in an agreement with the MD simulations and TEM observations [5–16]. However, nc metals and alloys exhibit a very low capacity for the dislocation storage during the uniform plastic deformation, as evidenced by the absence of the increase in the micro-strain [19], and by the recoverable full-width half-maximum (FWHM) of the X-ray diffraction patterns upon unloading [17].

The micromechanics of the plastic deformation of nc metals and alloys can be also studied by monitoring their intergranular residual stress as well as the associated residual lattice strain, ε_{hkl}, in different $h\,k\,l$ crystallographic planes. It is well established that the plastic deformation often introduces a grain-to-grain intergranular residual stress in the polycrystalline cg metals and alloys, due to the anisotropic elastic–plastic properties in different $h\,k\,l$ crystallographic planes of an individual grain in response to the applied macroscopic strain, ε_M [22–26]. When a plastic strain is accumulated, whether and how an intergranular residual stress at a grain level could be developed in the nc metals and alloys were not well studied [17,27]. The neutron-diffraction technique provides a powerful tool to investigate the intergranular residual-stress evolutions, as well as the associated texture developments during the plastic deformation of polycrystalline metals and alloys [22–26]. Furthermore, neutron can penetrate through bulk nc Ni–Fe alloys without causing any damage to samples, which is extremely helpful for studying bulk materials. While due to the limited neutron flux, large samples and long collection time will be required in neutron experiments. In this study, an in situ neutron-diffraction technique will be employed to study the uniaxial tensile plastic deformation of a bulk nc Ni–Fe alloy under cyclic loading and unloading. For comparison, experiments on a conventional cg Ni metal under the same loading and unloading condition will be performed.

The bulk nc Ni–18 wt.% Fe alloy with dimensions of 70 mm × 70 mm × 3 mm was produced using a pulsed-electrodeposition technique by Integran Technologies, Inc. Previous TEM observations indicate that the grain sizes of the as-deposited bulk nc Ni–Fe plate range from about 2–50 nm with an average value of about 23 nm [8]. The conventional cg Ni metal (99.99%) was purchased from Alfa Aesar. The samples were machined into dog-bone tensile specimens, and were polished for the in situ neutron-diffraction measurements. The tensile specimens have a gauge cross-section

* Corresponding author at: Smith International, Inc., MegaDiamond, 275 West 2230 North, Provo, UT 84604, USA.
E-mail addresses: gfan@smith.com, guojiang.fan@gmail.com (G.J. Fan).

0921-5093/$ – see front matter © 2008 Elsevier B.V. All rights reserved.
doi:10.1016/j.msea.2008.11.054

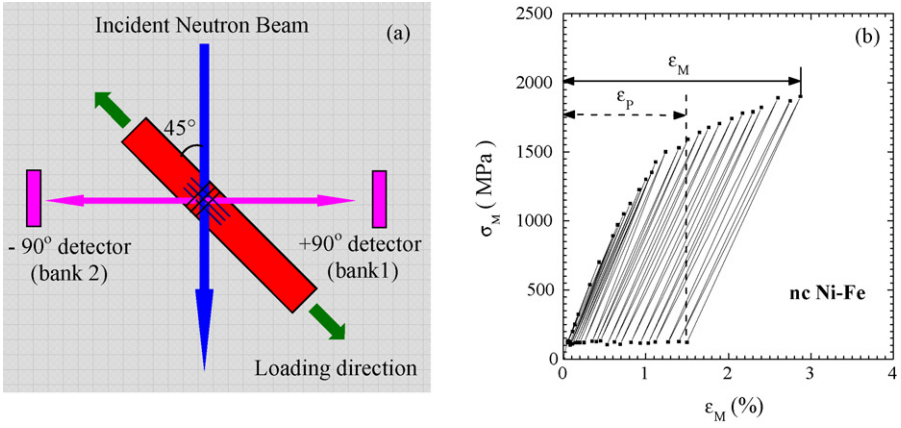

Fig. 1. The schematics of the in situ neutron-diffraction experiments using SMARTS (a), and the tensile macroscopic stress (σ_M)–macroscopic strain (ε_M) curve during the cyclic loading–unloading of a bulk nc Ni–Fe alloy (b). The neutron-diffraction patterns were recorded for 50 min when the sample was unloaded to about 100 MPa. The bulk nc Ni–Fe alloy fractured at macroscopic strain, ε_M = 2.9%, corresponding to a plastic strain, ε_P = 1.5%.

of 5 mm × 3 mm and a gauge length of 35 mm. In situ neutron-diffraction measurements were performed using the Spectrometer for Materials Research at Temperature and Stress (SMARTS) at the Lujan Neutron Scattering Center, Los Alamos National Laboratory. As shown in Fig. 1a, an incident neutron beam with beam size of 6 mm × 6 mm has a direction of 45° relative to the loading axis of the tensile specimens. The time-resolved spectra were measured by two detector banks (banks 1 and 2), which were centered on horizontal scattering angles of ±90°. The transverse and longitudinal diffraction patterns can be simultaneously measured by banks 1 and 2, respectively. Cyclic loading–unloading was performed during the uniaxial tensile test. A strain gauge was employed to monitor the macroscopic strain, ε_M. As shown in Fig. 1b, the samples were incrementally loaded at a strain rate of 0.02 s^{-1}, and were, subsequently, unloaded to about 100 MPa, where the neutron data were collected. To achieve a good statistics of the measured diffraction spectra, the samples were held for 50 min at each step. For the nc Ni–Fe alloy, the sample fractured at a plastic strain, ε_P, of 1.5% after 26 loading–unloading cycles. For the cg Ni metal, the sample did not fracture and the measurements were stopped after ε_P = 3.8%. It should be pointed out that the effects of loading frequency and the mean load during cyclic loading–unloading were not studied in this report, which requires further work to elucidate the issues.

A single peak analysis of respective hkl reflections was performed. The (1 1 1), (2 0 0), (2 2 0), and (3 1 1) peaks were analyzed by fitting a Gaussian function to the diffraction profiles, which yield the intensity and the FWHM of these diffraction peaks. The intergranular residual stress in different hkl crystalline planes causes a variation of the d_{hkl} spacing in the respective hkl diffraction peak. The residual lattice strain, ε_{hkl}, can be, therefore, calculated using $\varepsilon_{hkl} = (d_{hkl} - d^0_{hkl})/d^0_{hkl}$, where d^0_{hkl} is the d-spacing free from the residual stress [24].

Fig. 2 shows the diffraction intensity and FWHM of (1 1 1), (2 0 0), (2 2 0), and (3 1 1) peaks for both cg Ni and nc Ni–Fe as a function of ε_P. Note that the diffraction intensity and FWHM were normalized by the respective values of the samples free from the plastic deformation. Comparing Fig. 2(a) with (b), the normalized intensity of different diffraction peaks for the nc Ni–Fe alloy did not change obviously with increasing ε_P, whereas the normalized intensities of (1 1 1) and (2 0 0) peaks increase and the (2 2 0) peak decreases for the cg Ni with increasing ε_P. These results indicate that plastic deformation with ε_P < 1.5% did not introduce a texture in the nc Ni–Fe alloy. However, the (1 1 1) and (2 0 0) texture components were developed for the cg Ni, which agrees well with the previous reports [25]. It should be pointed out that the plastic deformation with a large ε_P (i.e., 5%) introduces a texture in the nc Ni–Fe alloy, particularly during the post necking plastic deformation, as studied by the ex situ high-energy ×-ray diffraction [19].

The normalized FWHM shown in Fig. 2(c) and (d) indicates that the normalized FWHM of the (1 1 1), (2 0 0), and (3 1 1) diffraction peaks decreases slightly with increasing ε_P for the nc Ni–Fe alloy, in contrast to the continuous increase with increasing ε_P for the cg Ni metal. The FWHM of the (2 2 0) diffraction peak of the nc Ni–Fe alloy shows a relatively large fluctuation. The plastic deformation of the polycrystalline metals, i.e., the cg Ni metal in this study, often leads to the peak broadening and a decrease in FWHM, which is attributed to the reduction in the grain sizes and/or to the increase in the dislocation density [28]. The observed decrease in FWHM for the present nc Ni–Fe alloy could be due to the increase in the grain sizes and/or to the reduction in the dislocation density. Recent studies indicate that the plastic deformation causes a grain growth in some nc metals and alloys [8,18–21,29,30], in contrast to the grain size reduction for the cg materials. Grain growth was also observed in the present bulk nc Ni–Fe alloy, as confirmed by the ex situ TEM observations. The ex situ TEM observations in the present bulk nc Ni–Fe alloys reveal that grains grow to about 60 nm after tensile test. This stress-induced grain growth in the nc metals and alloys has been attributed to the grain-boundary migration and/or grain rotation [8,18–21,28,29]. Since the plastic deformation of the nc metals and alloys unlikely causes a reduction in the dislocation density, the observed decrease in the FWHM of various diffraction peaks with increasing ε_P can be, therefore, attributed to the stress-induced grain growth in the nc Ni–Fe alloy.

The intergranular residual stress and the associated residual lattice strain often develop in the polycrystalline metals and alloys, since the deformation of the individual grains depends on crystallographic orientations, which are often anisotropic in the elastic–plastic properties [22–26]. For example, a very strong residual stress in a (2 0 0) plane was often observed in the face-centered cubic metals [25]. Fig. 3 shows the residual lattice strain, ε_{hkl}, in different hkl planes, as a function of ε_P for the cg Ni metal and the nc Ni–Fe alloy, respectively. As displayed in Fig. 3a, during the initial plastic deformation (ε_P < 0.1%), the ε_{200} increases rapidly for the cg Ni. Further plastic deformation leads to a continuous increase in ε_{200} to about 0.4×10^{-3}. An obvious residual lattice strain was also detected in the (2 0 0) and (3 1 1) planes. However, the plastic deformation did not introduce any obvious ε_{hkl} in all of the hkl crystallographic planes of the bulk nc Ni–Fe alloy (Fig. 3b). Together with variations of the normalized diffraction intensity and the FWHM shown in Fig. 2, these results imply that the deformation behaviors of the nc Ni–Fe alloy are different from those of the cg Ni. Finally, it should be mentioned that the development of ε_{hkl}

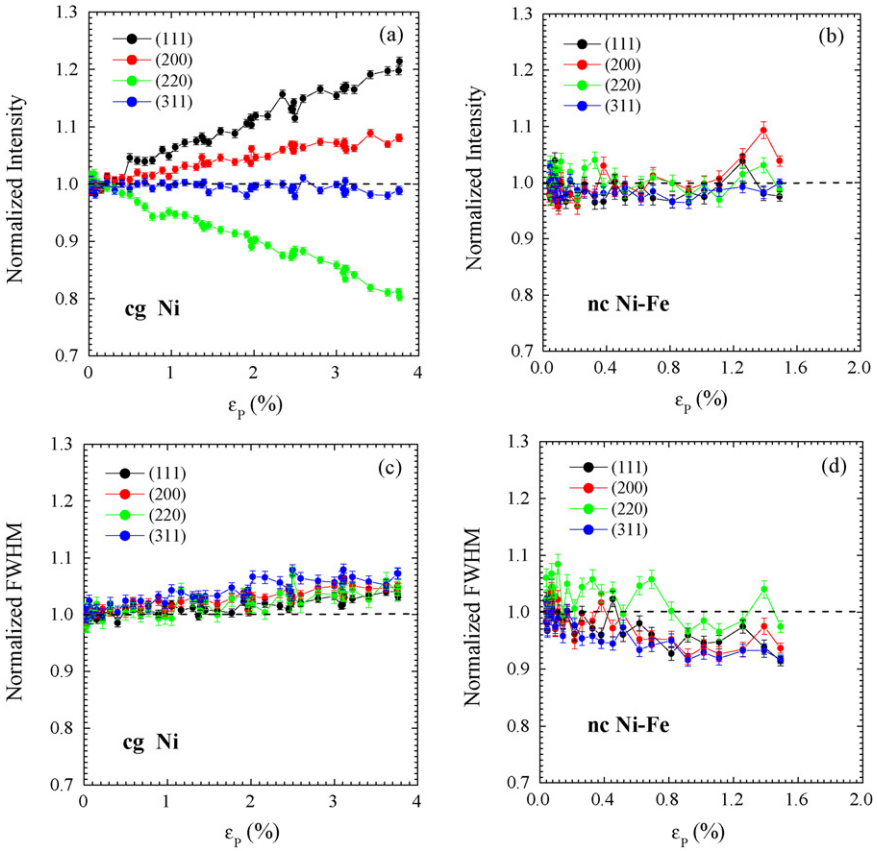

Fig. 2. The normalized intensity of the different diffraction peaks for the cg Ni metal (a) and nc Ni–Fe alloy (b), and the normalized FWHM for the cg Ni metal (c) and nc Ni–Fe alloy (d), as a function of the plastic strain, ε_P. The dashed lines in (a)–(d) are guided to eye.

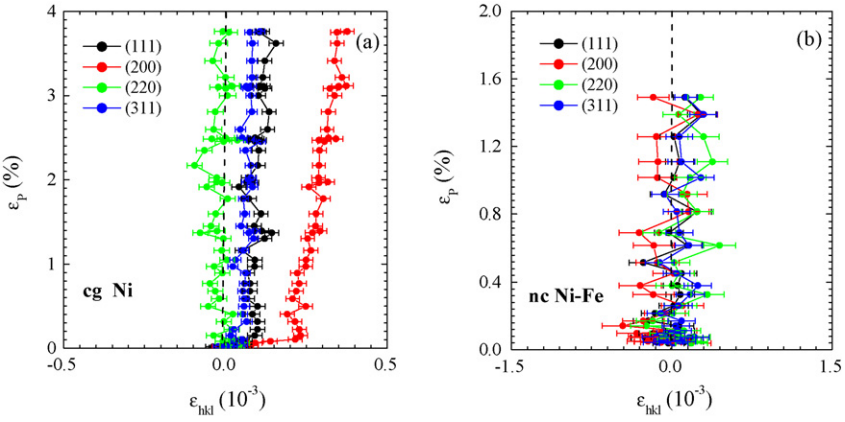

Fig. 3. The evolution of the residual lattice strain, ε_{hkl}, of different hkl crystallographic planes for the cg Ni metal (a) and nc Ni–Fe alloy (b) during the in situ neutron experiments. The dashed lines in (a) and (b) are guided to eye.

was reported by Budrovic et al. [17] in a nc Ni metal with an average grain size of 26 nm, and by Thilly et al. [27] in a Cu/Nb sandwiched nanocomposite, which was composed by a multiscale Cu matrix embedded by a Nd nanowire with a diameter of 267 nm. The origin of the absence of the ε_{hkl} in the bulk nc Ni–Fe alloy is not clear at the present stage. One possible explanation is that the ε_{hkl} developed during the plastic deformation of the nc metals could be simultaneously relaxed by the grain boundaries, which may exhibit a visco-elastic behavior [31].

In summary, the tensile plastic deformation of a bulk nc Ni–Fe alloy during the cyclic loading and unloading process has been investigated using an in situ neutron-diffraction technique. Meanwhile, a cg Ni metal during the same loading process has been studied and compared. The plastic deformation of the cg Ni leads to a texture development, an increase in the normalized FWHM, and an accumulation of the residual lattice strain. In contrast, the plastic deformation of the bulk nc Ni–Fe alloy with a plastic strain less than 1.5% did not introduce the texture and the residual lattice strain. A decrease in the normalized FWHM, due to the stress-induced grain growth, was observed in the bulk nc Ni–Fe alloy.

Acknowledgements

This work was supported by the National Science Foundation (NSF) International Materials Institutes (IMI) Program (DMR-

0231320). The authors thank the valuable discussion with Prof. Y.D. Wang of Northeastern University, China.

References

[1] R.Z. Valiev, R.K. Islamgaliev, I.V. Alexandrov, Progress in Materials Science 45 (2000) 103.
[2] G.W. Nieman, J.R. Weertman, R.W. Siegel, Journal of Materials Research 6 (1991) 1012.
[3] C.A. Schuh, T.G. Nieh, H. Iwasaki, Acta Materialia 51 (2003) 431.
[4] R.Z. Valiev, I.V. Alexandrov, Y.T. Zhu, T.C. Lowe, Journal of Materials Research 17 (2002) 5.
[5] Y.M. Wang, M.W. Chen, F.H. Zhou, E. Ma, Nature 419 (2002) 912.
[6] K.S. Kumar, S. Suresh, M.F. Chisholm, J.A. Horton, P. Wang, Acta Materialia 51 (2003) 387.
[7] G.J. Fan, H. Choo, P.K. Liaw, E.J. Lavernia, Acta Materialia 54 (2006) 1759.
[8] G.J. Fan, L.F. Fu, H. Choo, P.K. Liaw, N.D. Browning, Acta Materialia 54 (2006) 4781.
[9] X.Z. Liao, F. Zhou, E.J. Lavernia, S.G. Srinivasan, M.I. Baskes, D.W. He, Y.T. Zhu, Applied Physics Letters 83 (2003) 632.
[10] M.W. Chen, E. Ma, K.J. Hemker, H.W. Sheng, Y.M. Wang, X.M. Cheng, Science 300 (2003) 1275.
[11] K.M. Youssef, R.O. Scattergood, K.L. Murty, J.A. Horton, C.C. Koch, Applied Physics Letters 87 (2005) 091904.
[12] Z.W. Shan, E.A. Stach, J.M.K. Wiezorek, J.A. Knapp, D.M. Follstaedt, S.X. Mao, Science 305 (2004) 654.
[13] R.C. Hugo, H. Kung, J.R. Weertman, R. Mitra, J.A. Knapp, D.M. Follstaedt, Acta Materialia 51 (2003) 1937.
[14] H. Van Swygenhoven, P.M. Derlet, Physical Review B 64 (2001) 224105.
[15] D. Wolf, V. Yamakov, S.R. Phillpot, A. Mukherjee, H. Gleiter, Acta Materialia 53 (2005) 1.
[16] J. Schiotz, F.D. Di Tolla, K.W. Jacobsen, Nature 391 (1998) 561.
[17] Z. Budrovic, H. Van Swygenhoven, P.M. Derlet, S. Van Petegem, B. Schmitt, Science 304 (2004) 273.
[18] G.J. Fan, Y.D. Wang, L.F. Fu, H. Choo, P.K. Liaw, Y. Ren, N.D. Browning, Applied Physics Letters 88 (2006) 171914.
[19] G.J. Fan, L.F. Fu, Y.D. Wang, Y. Ren, H. Choo, P.K. Liaw, G.Y. Wang, N.D. Browning, Applied Physics Letters 89 (2006) 101918.
[20] D.S. Gianola, S.V. Petegem, M. Legros, S. Brandstetter, H. Van Swygenhoven, K.J. Hemker, Acta Materialia 54 (2006) 2253.
[21] X.Z. Liao, A.R. Kilmametov, R.Z. Valiev, H.S. Gao, X.D. Li, A.K. Mukherjee, J.F. Bingert, Y.T. Zhu, Applied Physics Letters 88 (2006) 021909.
[22] E.C. Oliver, M.R. Daymond, P.J. Withers, Acta Materialia 52 (2004) 1937.
[23] D.W. Brown, M.A.M. Bourke, B. Clausen, T.M. Holden, C.N. Tome, R. Varma, Metallurgical Materials Transactions 34A (2003) 1439.
[24] H. Choo, D. Seo, J. Beddoes, M.A.M. Bourke, D.W. Brown, Applied Physics Letters 86 (2004) 4654.
[25] N. Jia, R.L. Peng, Y.D. Wang, G.C. Chai, S. Johansson, G. Wang, P.K. Liaw, Acta Materialia 54 (2006) 3907.
[26] Y.N. Sun, H. Choo, P.K. Liaw, Y.L. Lu, B. Yang, D.W. Brwon, M.A.M. Bourke, Scripta Materialia 53 (2005) 971.
[27] L. Thilly, P.O. Renault, V. Vidal, F. Lecouturier, S. Van Petegem, U. Stuhr, H. Van Swygenhoven, Applied Physics Letters 88 (2006) 191906.
[28] H. Mughrabi, Plastic Deformation and Fracture of Materials, vol. 6, Wiley–VCH, Weinheim, Germany, 1991, p. 1.
[29] K. Zhang, J.R. Weertman, J.A. Eastman, Applied Physics Letters 85 (2004) 5197.
[30] M. Jin, A.M. Minor, E.A. Stach, J.W. Morris, Acta Materialia 52 (2004) 5381.
[31] G.J. Fan, H. Choo, P.K. Liaw, E.J. Lavernia, Metallurgical Materials Transactions 35A (2005) 2641.